Development of a low-cost movable hot box for a preliminary definition of the thermal conductance of building envelopes

(Article begins on next page)

28 December 2024

Development of a low-cost movable hot box for a preliminary definition of the thermal conductance of building envelopes

A. Barbaresi[a]*, M. Bovo[a], E. Santolini[a], L. Barbaresi[b], D. Torreggiani[a], P. Tassinari[a]

[a]*Department of Agricultural and Food Sciences (DISTAL) – University of Bologna*
Viale G. Fanin, 48 – 40127 Bologna, Italy

[b]*Department of Industrial Engineering (DIN) – University of Bologna*
Viale del Risorgimento, 2 – 40136 Bologna, Italy

* Corresponding author. E-mail: alberto.barbaresi@unibo.it - Viale G. Fanin 48 – *40127 Bologna, Italy*

ABSTRACT

In the recent years, very promising solutions are available for energy-efficient building envelope. Particular interest is risen by the use of innovative natural or bio-based materials. Even if, in some cases, they are wastes coming from industrial or agricultural processes, they can be effectively applied as by-product for the creation of new more sustainable insulation panels and composite materials. In this context, the thermal characterization of a new building material, actually need of very expensive equipment, with fixed installation, requiring expensive usage and periodic calibration and maintenance. Development of alternative methodologies to determine thermal properties, even in a preliminary way, seems important in order to reduce the cost and to make the tests accessible to wider number of researchers. This paper describes the development and the validation test of a low-cost movable hot box suitable for a preliminary assessment of the thermal conductance of wall elements and insulation panels with dimensions about 1m×1m. The prototype of the hot box has been realized and then tested in the conductance range 0.5-10 W/(m^2 K) by adopting two commercial panels used in the building sector. The availability of a low-cost, low-size and moveable equipment allowing a quickly and preliminary assessment of the thermal characteristics of a by-product is useful to understand if the material has suitable properties for future re-use. All this allows the reduction of laboratory time and costs needed for the thermal characterization tests.

Keywords: building envelope; thermal conductance; agricultural waste; guarded hot box; calibrated hot box

SYMBOLS AND UNITS

Symbol	Quantity	Unit
λ	design thermal conductivity	W/(m·K)
Λ	thermal conductance	W/(m²·K)
U	thermal transmittance	W/(m²·K)
q	density of heat flow rate	W/m²
T_{si}	interior surface temperature	K
T_{se}	exterior surface temperature	K
Φ	heat flow rate	W
A	area	m²
R	thermal resistance	(m²·K)/W
D_T	test duration	d (days)
t	thickness	mm

1. INTRODUCTION

The United Nation Environment Program [1] estimated that buildings sector is responsible for 40% of world global energy consumptions, 25% of the global water and 40% of the global resources. With approximately 35% of buildings over 50 years old, the sector notices the painful record of first producer of greenhouse gas emissions (e.g. the 36% of CO_2) [2,3]. Boosting a deep renovation of the building sector, involving all the processes from the production to the disposal, is one of the most compelling challenges. The sustainability of the sector can be increased by means of two different approaches: on one hand by reducing the impacts of production phase (e.g. by reducing the wastes, the consumptions, the use of raw materials etc.) [4,5] on the other hand, by decreasing the energy needs during the service life (e.g. replacing existent elements with other with better performances, lowering the running costs etc.) [6]. In this context, very promising applications are coming from the use of innovative building envelopes based on low-cost materials like, for example, the wastes coming from industrial or agricultural processes. In fact, even if considered wastes of other supply chains, different materials can be effectively applied for the production of insulation panels [7–9] or be introduced in the mixtures of traditional building materials [10,11] in order to improve their performances. With the introduction of these low-cost materials, a double benefit can be obtained, given that, first of all reducing the waste amount to dispose and, second of all, saving raw materials. To this regard, the by-products must be carefully selected and then characterized based on the feasible applications, since they could present a large property variability. Recent studies demonstrated the bio-based materials play a fundamental role in a sustainable architecture. Showing remarkable thermal performance [12], bio-based materials are more and more used in energy-efficient buildings but, differently to materials with same thermal properties, they enhance the effectiveness of sustainable architecture having a reduced carbon footprint [13,14].

Then, in the context of building thermal insulation (by using nomenclature and symbol of ISO 9869-1:2014 and ISO 6946) [15,16], the design thermal conductivity λ [W/(m·K)] of a material and the thermal transmittance U [W/(m²·K)] or the thermal conductance Λ [W/(m²·K)] of an envelope are among the most important properties to define based on the intended use of the building [17]. In fact, most of the energetic performances of a building could be directly or indirectly correlated to the performance of the envelope materials [18,19]. The thermal conductance Λ can be defined as the heat flow rate in the steady state condition divided by the transmitting area and by the temperature difference between the surfaces on each side of a system.

With regard to procedures suggested by the CEN - EN ISO 8990 and ASTM C518 [20,21] two different apparatus are suggested for the characterization of the thermal transmission properties of an envelope element (or envelope portion): the guarded hot box (GHB) and the calibrated hot box (CHB). In both the systems, the specimen is placed between a hot and a cold chamber in which environmental temperatures are known. The structures and equipment necessary for the realization of a GHB or a CHB are typically expensive to implement, require periodic calibration and maintenance and, being unmoveable, need of a permanent dedicated area usually obtained within a laboratory. Given their high implementation and management costs and the difficulties to insert into the layouts of existing laboratories, these types of apparatus are not widespread. Furthermore, also the preparation of a test in a GHB or a CHB chamber need considerable costs, takes a considerable time and requires the production of large samples. Development of alternative methodologies to determine thermal properties, even in a preliminary way, seems important in order to reduce the experimental campaign costs and to make the tests accessible to wider number of researchers, public and private laboratories, professionals, constructors and companies in general.

Other investigators developed analogous systems for laboratory evaluation of the building material thermal performances. For example, Gounni et al., 2019 [22] used a thermally-

controlled reduced-scale cavity for the evaluation of insulation materials based on textile waste. Using two climatic chambers, Ricciu et al. 2018 [23] performed full-scale experimental measurements of conductivity, specific heat, time lag and attenuation factor for lightweight materials. However, the former solution can be affected by the scaling effects due to the reduced dimensions of the sample, while the latter climatic apparatus could result quite complex to relocate since the two control chambers move on rails.

Then, Meng et al. [24,25] proposed the Simple Hot Box - Heat Flow Meter (SHB-HFM) method, to be used for measuring the wall thermal transmittance in situ, avoiding both the use of GHB/CHB equipment and the limitation of the heat flow meter method strongly dependent from the outdoor and indoor thermal environment. An improved SHB-HFM method is described and proposed in Roque et al. [26]. In the improved SHB-HFM device, based on the procedure described in the standard ISO 9869-1:2014, a baffle was introduced between the heat sources and the wall in order to control the radiative part of the heat transfer on the heat flow meters. Both these two solutions proved to be effective for the desired objectives maintaining at the same time simplicity and portability for in situ test. Although in some circumstances in situ tests are unavoidable, laboratory tests conducted in similar conditions can be more accurate due to the higher precision and control of the various parameters, both environmental and in the preparation of the specimens to be tested.

For what said, the present work aims to describe, develop and test a movable hot box (MHB), for laboratory purposes, for the determination of the conductance of insulation panels or even of the whole wall envelopes.

The MHB presented here is a cube box (1m of edge), realized with five oriented strand board (OSB) panels insulated with expanded polystyrene (EPS) where the element to be characterized is placed in the frontal (empty) face of the cube. The conductance value is obtained starting from the measurements of the outlet heat flow from the apparatus recorded with heat flow meters mounted on the panel of material to be tested. The design and

construction of the hardware, and the software implementation allowing the data acquisition and processing, are widely described in the following Section 2.

In order to validate the realized MHB prototype, two commercial materials have been used: a high conductance material (OSB panel) and a low conductance material (EPS). The main results obtained with the MHB on the two materials have been reported in Section 3, in terms of conductance, and the identified values have been compared with those of a calibrated lab test machine. Moreover, the experimental tests have been reproduced also with computational fluid dynamics simulations confirming the outcomes reliability.

The availability of a low-cost, low-size and moveable equipment, allowing a quick assessment of the thermal characteristics of a material, is useful to preliminary assess the suitability of its thermal properties as building envelope material.

The MHB ~~presented here~~ has been originally conceived in order to preliminary characterize the thermal properties of bio-based materials, also considering waste products, since several recent researches have investigated this material class [12,27–31] showing the high potentialities. For these applications, also a rougher evaluation of the thermal properties could be sufficient, since due to the natural origin of the materials, large variability is expected even if the samples are well-prepared and base components have been well-selected. Nevertheless, the present device could be theoretically applied to generic material classes.

As far as the uncertainty of the heat flow meter method is concerned [15] the scientific literature reports that most important aspects to consider are: the temperature difference (T_{si}-T_{se}) between internal and external surfaces [33–35], the heat flow gradients [36] the environmental temperature oscillations [37] and the air humidity variations [33]. Some suggestions aiming to reduce the uncertainty in HFM method can be found in the ISO 9869-1:2014 and in literature [38,39]. The importance of achieving a proper T_{si}-T_{se} value, i.e. higher than 10°C, is maybe the most emphasized, since increasing the T_{si}-T_{se} reduces the negative effects of the temperature fluctuations and thus increases the accuracy of the measurements.

Moreover, Trethowen [40] highlighted that a better measurements accuracy is achieved if T_{si} is kept as constant as possible.

All this is extremely positive for the MHB applications since both the temperatures inside the box and in the surrounding environment can be usually and easily controlled within a laboratory. The adoption of devices, like the MHB, allows the reduction of time and costs needed for the envelope thermal characterization in laboratory.

2. MATERIALS AND METHODS

The present Section starts with a short review of the prescriptions in current International codes relative to thermal characterization of plane building components, then presents the description of the Computational Fluid Dynamics (CFD) analysis adopted for the preliminary sizing. Then the Section describes the main components of the apparatus proposed here: the hardware of the case, the sensors for measurements and security control ~~check~~ and the software for data acquisition and processing.

2.1 *International standards for material thermal characterization*

The evaluation of thermal performance of both components and materials is becoming a delicate matter in the building sector, especially with reference to insulation, since on one hand the procedures adopted must guarantee the application of the International Directive [41] to achieve a more rational use of energy resources but, on the other hand, it should not require such strict prescriptions and expensive apparatus so to discourage experimentation and research on the subject.

To this regard, following the ISO 8301 approach [42], the actual heat transfer within insulation materials can involve a complex combination of different contributions of radiation, conduction and convection and their interaction. Therefore, the heat transfer, may be not an intrinsic property of the material itself (it may have, for example, significant dependence on specimen

7

thickness, temperature difference for the same mean test temperature, apparatus orientation and other factors such as workmanship) and general rules valid for all insulation materials are hard to be defined.

In the evaluation of the in-laboratory thermal performance of building materials and products, the determination of thermal resistance – by means of guarded hot plate and heat flow meter methods [43] on small scale samples (e.g. 40cm×40cm or 50cm×50cm) – results a very common procedure for homogeneous materials, but not applicable to the most of the non-homogeneous elements.

On the other hand, the GHB and CHB apparatus suggested by the EN ISO 8990 [20] for large scale specimens (larger than 150cm×150cm) actually results very expensive and request a fixed installation within a laboratory. Furthermore, as far as the accuracy of the tests is concerned, experience has shown that an accuracy within $\pm$ 5 % can generally be achieved when testing homogeneous specimens following the indications in EN ISO 8990 [20]. Lower accuracy results can then be expected for non-homogeneous materials and elements.

The in-situ measurement of thermal resistance and/or thermal transmittance of building insulating elements can be even more complicated and International standard concerning this matter, provides useful insight into this problem. In fact, ISO 9869-1:2014 [15] underlines that the steady-state conditions practically never occur on a site, therefore the definition of the measurement of thermal transmittance as provided by the ISO 7345 [44] is usually not possible. Then, EN ISO 7345:2018 [44] suggests alternative ways to solve this issue, by in-situ measurements. For example, assuming that the mean values of the heat flow rate and temperatures – over a sufficiently long period of time – give a good estimation of the steady-state values, or by using a dynamic theory considering heat flow rate and temperatures fluctuations in the analysis of the acquired data. Nevertheless, the first solution is valid only if the element properties and the heat transfer coefficients are constant over the range of temperature fluctuations measured during the test and the amount of heat stored in the

element is negligible when compared to the amount of heat going through the element. Moreover, ISO 7345 [44] describes two alternatives methods, less precise than the method cited before using the GHB/CHB instruments, but able to provide a reliable approximation. For plane building opaque components, the heat flow meter (HFM) method, can be effectively applied for the measurement of thermal transmission properties perpendicular to the heat flow if no significant lateral heat flows are present. In this context, the thermal conductance Λ of the building element, surface to surface, can be calculated by the following Eq.(1):

$$\Lambda = q / (T_{si} - T_{se}) \tag{1}$$

where: q is the density of heat flow rate $= \Phi / A$; T_{si}, T_{se} respectively are the internal surface temperature of the building element and external surface temperature, both in °C or K; Φ is the heat flow rate and A the area crossed by Φ.

The alternative for in-situ measurement is the infrared method proposed by the ISO 9869-2:2018 [32]. This method is a valid alternative to the more precise in-laboratory test on hot box apparatus. Two methods may be used for analysing the data in accordance with this part of ISO 9869-1:2014 the so-called "average method" or the "dynamic method".

Finally, the ISO 9869-1:2014 prescribes very strictly conditions in order to guarantee a sufficient test accuracy and convergence of the method.

Obviously, these strict conditions are thought coming from in-situ measurement in order to properly consider the effects of the daily oscillation on outdoor temperature. Naturally, if one day (24h) represent one entire cycle, by introducing at least three temperature cycles (minimum 72h of test) U can be considered as a three-day average measure. Then, an important aspect, to keep in mind when carrying out experimental tests with HFM, is that in general all the results are affected by errors of various nature (e.g. measurement errors, model errors etc.). Following the indications in the ISO 9869-1:2014 the total uncertainty of the measurement can be expected in the range from 14% to 28%.

Concluding, with the current procedures, the thermal properties of building elements (panels for insulation, wall panels etc.) could be estimated in-situ with uncertainty rather large, approximately around ±20%, and this threshold therefore seems, reasonably, acceptable also for a low-cost preliminary test having the purpose of identifying potential high-performance materials to test with more precise and expensive methods in a second phase.

2.2   *CFD modelling and analyses*

The gross sizing of the dimensions to adopt for the MHB was performed on the basis of the outcomes of ~~a series of~~ preliminary CFD analyses having the main goal to evaluate the heat convection process inside the apparatus. For this, a 3D model of the MHB was adopted and carried out by Autodesk Inventor 2018 [45] and then analysed by means of CFD simulations with the software STAR CCM+ [46]. During the sizing process different dimensions for the MHB were considered. The most suitable edge length of the MHB has been identified as the minimum edge length providing a 1-dimensional heat transfer surface, allowing to test the same specimen in several representative positions. In this way, a statistical characterization of the expected conductance variance can be achieved. This aspect is especially important when heterogeneous materials – with high variability characteristics – must be tested. The suitable surface (surface characterized by 1-dimensional heat transfer) has been identified with the criterion of the parallel direction of the isotherms (i.e. the area where the isotherms on the sample thickness assume a parallel direction). Therefore, when more than one measurement is necessary for statistical needs (i.e. loose or non-uniform materials), tests can be performed measuring specimen points 30-40 cm distant one from each-other.

For the cube MHB device, have been considered different edge dimensions ranging from 2.5m to 0.75m. The first simulation considered a cube box with edge around 2.5m and, progressively, the dimensions of the box were reduced. For each edge dimension the suitable area that respects the above cited criterion has been identified. From the preliminary CFD simulations,

we obtained that the minimum edge length, necessary to guarantee a suitable area of specimen for the monitoring of temperatures and heat flow was about 1 meter. So, we considered this dimension as the optimal for the MHB prototype. For the sake of brevity only the description of the final model, with 1meter edge length achieved at the end of the progressive hot box dimension reduction, has been described in the following. In the CFD simulations, ~~we considered~~ a simplified analyses representative of several possible future application of the box has been considered.

The final model presents a whole domain of 6m × 6m × H=4m with at the center the 1 m³ MHB, which has been modelled as not hermetically closed. In fact, the air circulation is slowed by an open frame of 1 mm at the lateral and top side. The inlet has been defined in front of the box and the other boundaries of the solution domain have been set as pressure outlet. In the model, six identical faces, realized with OSB panels 18mm thick insulated with panels of EPS with 80 mm of thickness, have been assumed. The MHB walls have been modelled with the specific properties of the materials, i.e. EPS and OSB, as extracted by producer spreadsheets or obtained by laboratory tests when missing or uncertain. In this way the real properties of the materials have been considered on the heat exchange between inside and outside of the box. The materials assumed in the simulations are the same adopted for the realization of the prototype. The *k-epsilon* model has been used in the simulations, performed in unsteady-state conditions with a numerical time step of 20s. The heat source, i.e. the 1000 w heater inside the MHB, has been defined. The initial conditions in the volume around the device (i.e. a research laboratory) have assumed as follows: air velocity equal to 0.05 m/s and air temperature value of 21°C. In the simulations, the temperature value at the center of the MHB device was the check parameter. The target temperature has been set equal to 45 °C. The simulations have been stopped after 500 iterations, when the temperature inside the box reached the target value. As an example, the 3D model of the MHB with edge length of 1 meter is showed in Figure 1a. Firstly, four different meshes have been solved in order to conduct the grid convergence study based

on one case [47,48]. The grids have been carried out by polyhedral mesh progressively refined, from $3e^6$ to $26e^6$ number of cells (value related to the case of MHB with edge length equal to 1 meter). The Figure 1b shows, the results of the convergence study for the model with edge length equal to 1meter, where the independency of the results from the grid has been reached at the third refinement of the mesh considering $13e^6$ cells.
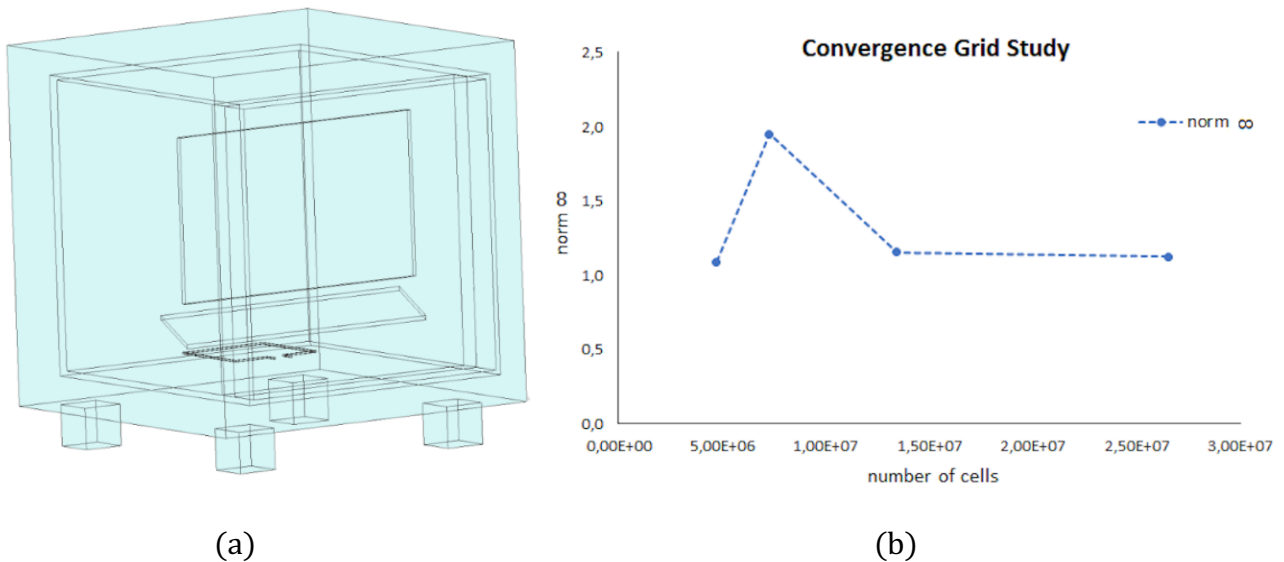

| (a) | (b) |

Figure 1. CFD simulations for the study of the MHB with edge length of 1 meter. (a) 3D geometrical model. (b) Convergence study on the grid performed using the infinity norm as reference.

After the gross sizing of the main dimensions of the apparatus based on preliminary CFD simulations, a prototype with edge dimension about 1 meter was realized and described in the following subsections. Further results of the CFD simulations are reported in the Results and Discussion Section where the numerical models, after a refinement, were used as a tool for the validation of the MHB functioning. The transparent view in Figure 1a allows to see two internal screens, one vertical and one inclined. These two elements prevent the front panel – where the sample to be characterized must be positioned – from the direct internal radiation generated by the heater and from direct air flow produced by the fan. The exact positions and dimensions of these two important components are properly described in the following subsection.

2.3   *Hardware design and construction*

The structure of the MHB presented here is a cube box, about 1m of edge, realized with five OSB panels 18mm thick insulated with panels of EPS with 80 mm of thickness. The MHB is depicted in Figure 2.
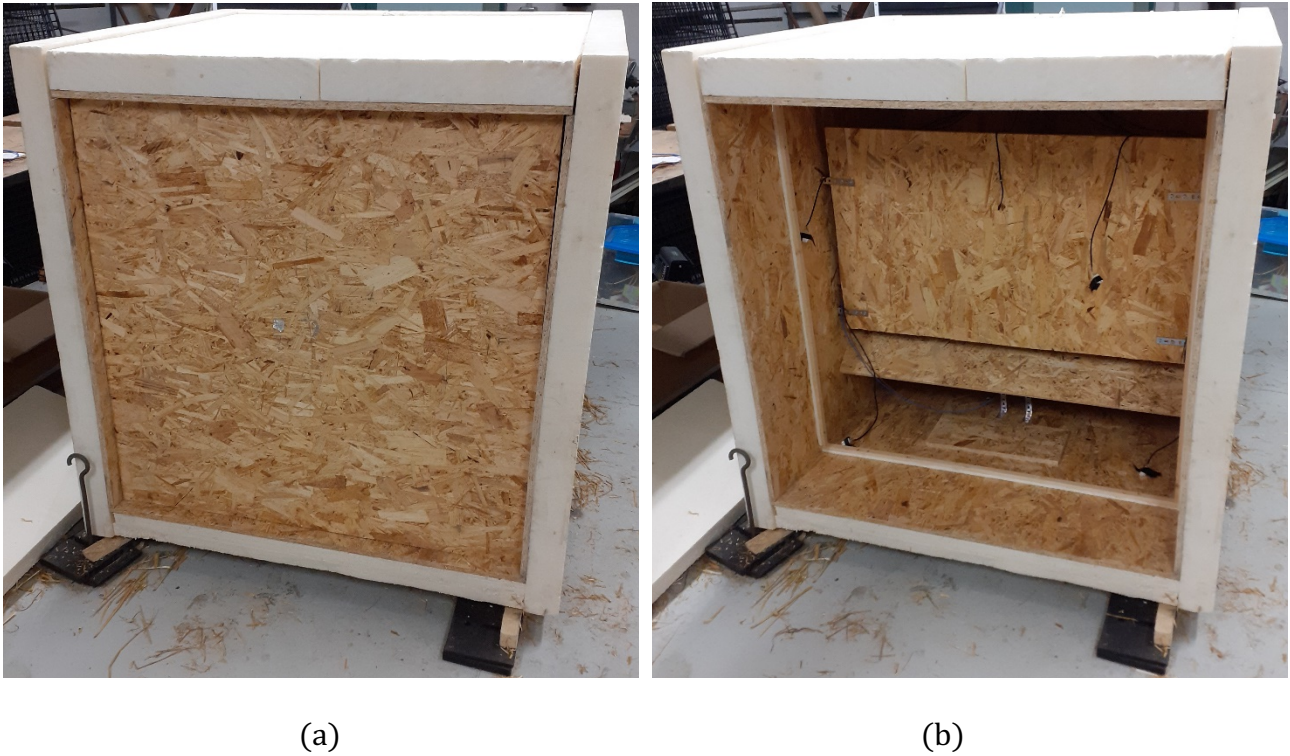

(a)   (b)

Figure 2. The movable hot box (MHB). (a) With a sample element and (b) without the sample element installed.

A global 3D sketch of the MHB is reported in Figure 3 together with the components' details. The main box (P1) has a removable lid (P2) to allow the sample housing and the installation of the various sensors. The frontal (empty) face of the box houses the element to be thermal characterized. To heat up air inside the box a thermal resistance (P3), a Candy oven lower heater hoover Zerowatt 1050, was introduced (see details in Figure 4a).
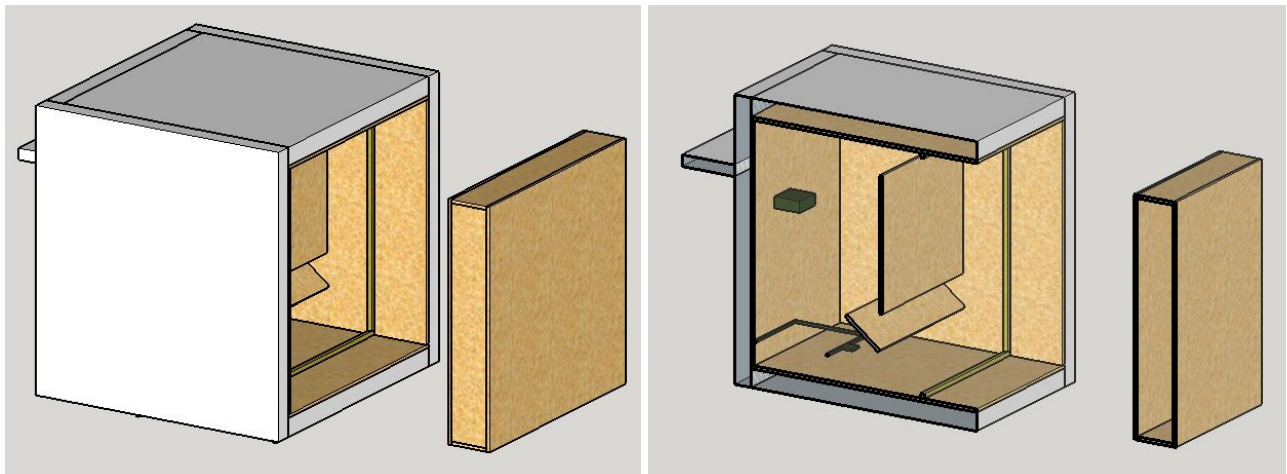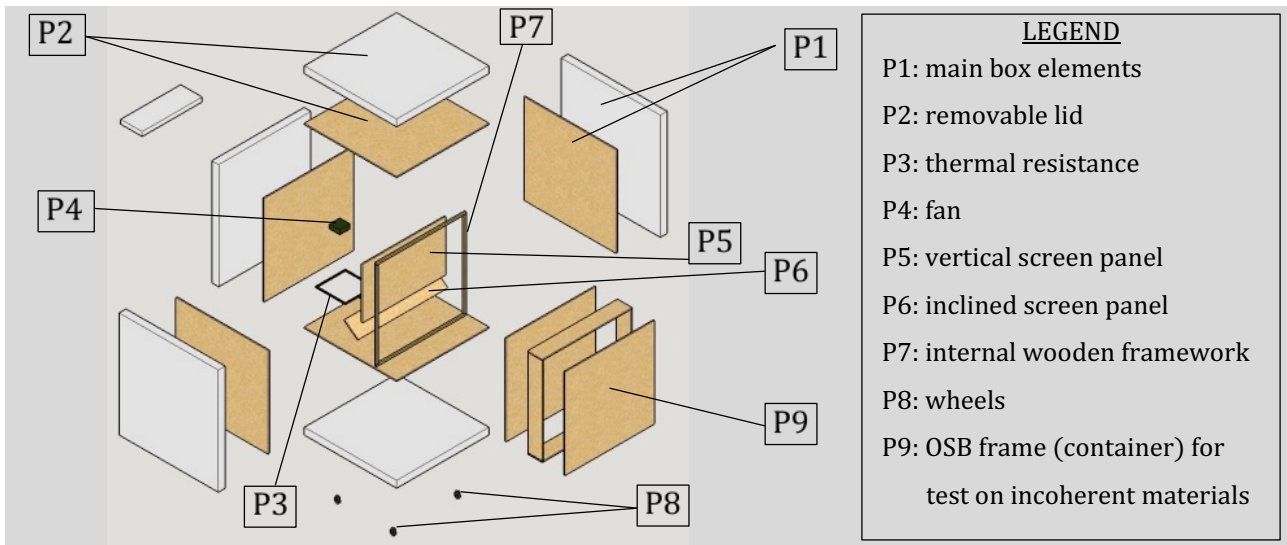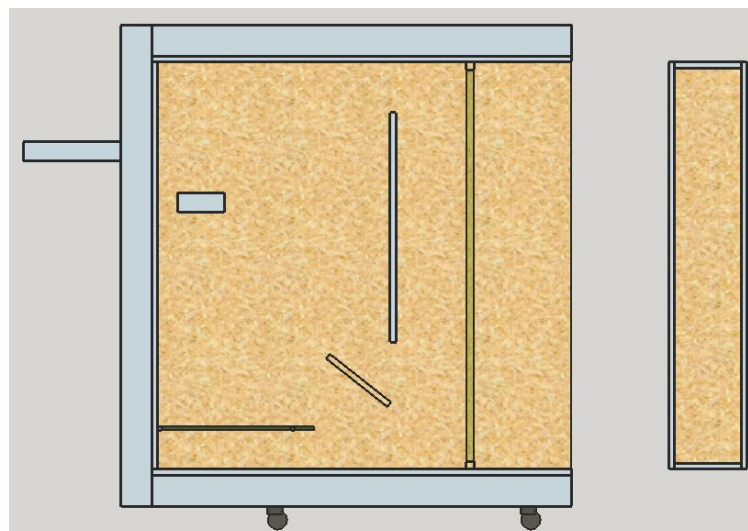
Figure 3. Design of MHB. (a) Global 3D view. (b) Axonometric inner view. (c) Exploded view with indicated the main components. (d) Vertical transversal section.

LEGEND

P1: main box elements

P2: removable lid

P3: thermal resistance

P4: fan

P5: vertical screen panel

P6: inclined screen panel

P7: internal wooden framework

P8: wheels

P9: OSB frame (container) for test on incoherent materials

Moreover, to guarantee a homogeneous air temperature inside the box, a fan (P4), Axial AC Fan Model RAH 1225S1 with vertical axis, was positioned above the resistance (see details in Figure 4b). Inside, the volume of the box has an OSB vertical panel (P5) and an inclined panel (P6) preventing the sample from the direct internal radiation generated by the electrical resistance and from direct air flow. Specifically, to avoid the radiation problem, the box is internally made by the same low-emissivity material (OSB) and an OSB panel has been placed between the heater and the application area of the flow meter (that is also protected by a reflecting tape), paying attention that flow meter is completely screened from direct and reflected radiations. Additional temperature measurements demonstrated the screen panel and other non-screened surfaces did not show temperatures higher than the one recorded close the flow meter, entailing that the flow meter is not affected by heater radiations.

The box results to have a global weight about of 0.5 kN and results very easy to move since wheels are installed at the bottom. The empty face (front) of the wall, was studied to properly house the element to test. To this regard an internal wooden framework covered by an insulating thermoplastic adhesive profile (P7), connected to the main box (P1), has been realized so as to provide a suitable housing for the element that limits as much as possible the drafts between the internal volume of the box (the hot chamber) and the surrounding volume (the cold chamber, at room temperature). Four wheels (P8) allow the easy movement of the box. The equipment was designed to test not only self-carrying panels but also incoherent of infill materials coming from agriculture and industrial processes. Typically, they have loose consistency so, a frame made with OSB panels was created (P9) and used to hold the materials to be characterized. The element P9, properly filled and closed, or the panel to test, must be pushed against the frame P7 on the empty face of the box. In detail, the samples, must have the following dimensions: height 103 cm ($\pm$1.5 cm), width 103 cm ($\pm$1.5 cm) , thickness up to 20 cm. Self-supporting one-layer or multilayer specimens can be directly inserted on the chamber, and must adhere to the internal frame (see Figure 3c, P7) to avoid air leakage, the gap between

the chamber and possible irregular borders is filled with neoprene or insulating foam to avoid thermal bridges. A specific container, made by OSB frames and panels, are realized to test loose and incoherent materials. The container can be built with different frames according to desired thickness. The container panels have been tested to assess their thermal performance, therefore their contribution during the test. Flexible materials can be supported by a steel wireframe or, if the structure affects the test, can be inserted in the container. Preliminary tests on 2 kN specimens did not caused any damage to the chamber. Further tests will be carried out in the future.
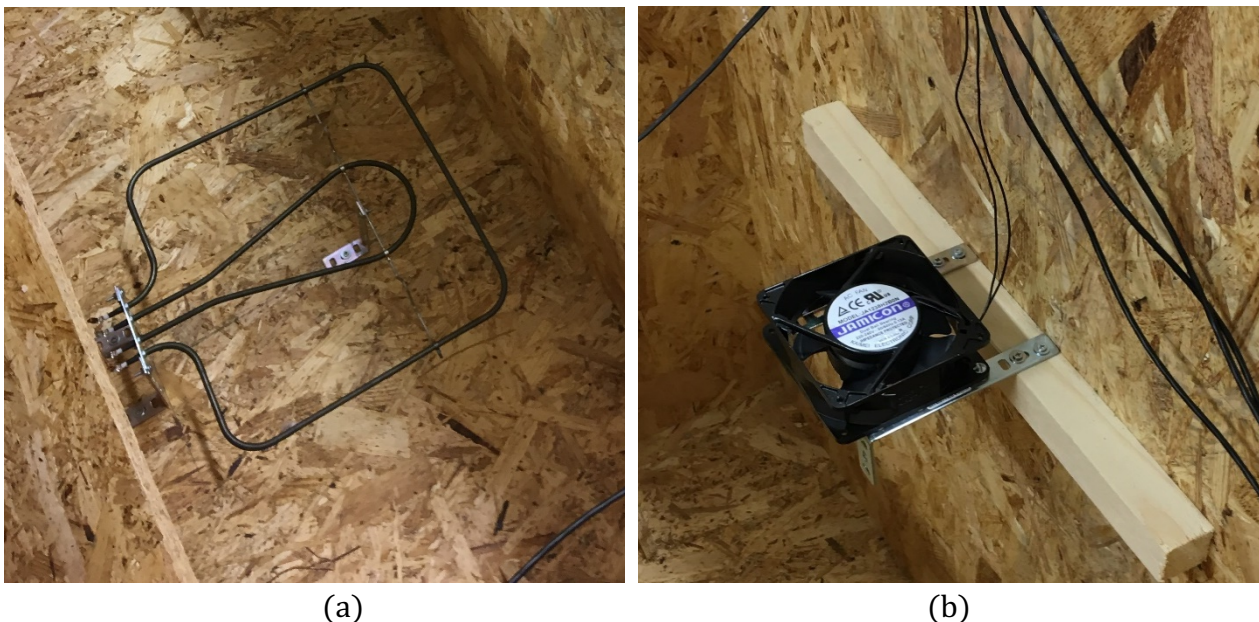

| (a) | (b) |

Figure 4. Some details of the MHB components. (a) Thermal resistance. (b) Fan.

2.4   *Sensors and hardware control*

The main aim of the box is to create a proper environment for the tests. Specifically, it should guarantee a uniform internal temperature (overall where the test face is placed) at least 10-15°C higher than the room temperature for a circa 3-day time duration.

The proper internal environment can be create using a heater (i.e. thermal resistance) to rise the temperature, and a fan to ease the uniformity in the temperature distribution. Finally, temperatures must be recorded allowing the post-processing-analysis.

Due to the operative time for a single test (until 72 hours), the system should be provided with a control system able to control the heater and the fan (and so the internal temperature), to record data, to display the main data and warnings, shut off the system in case of emergency.

The required operations are relatively simple; therefore, an Arduino board was chosen for the control unit (see Figure 5). Besides Arduino, the control system is made by a heater (1000W-220V thermal resistance), a fan (220VAC), two relays (2Ch DC 5V), a 4×20 display (I2C Serial 2004 20x4 LCD Display), a SD board, a clock RTC1302, and six DHT22 temperature-humidity sensors (with ± 0.5°C of temperature accuracy and ± 2% humidity accuracy). One sensor is placed out of the box to record environmental data (in our case the indoor thermo-hygrometric conditions of the lab). The remaining five sensors are located internally close to the tested panel side: four were15 cm far from the corners and one in the center panel. This arrangement has been thought in order to check the uniformity of temperature distribution.

The positioning of heater and fan has been defined according to CFD analysis and on-site tests. Sensors are connected directly to the main board, heater and fan to the relays commanded by the board. Finally, the RTC, display and recording SD board too are connected to Arduino. The hardware is completed by a Optivelox Thermozig BLE [49] device. The Thermozig BLE is mainly composed by:

- a wireless data logger DL02 (500 000 records available; 16 bit of data resolution);

- a wireless heat flow meter sensor (with accuracy ±5% at T=20°C).

Then, the data logger has been used to record the data from the flow meter sensor and the SD board, on ARDUINO, recorded the data of the six temperature-humidity sensors.

In addition, an emergency system can stop the power supply as better explained later.
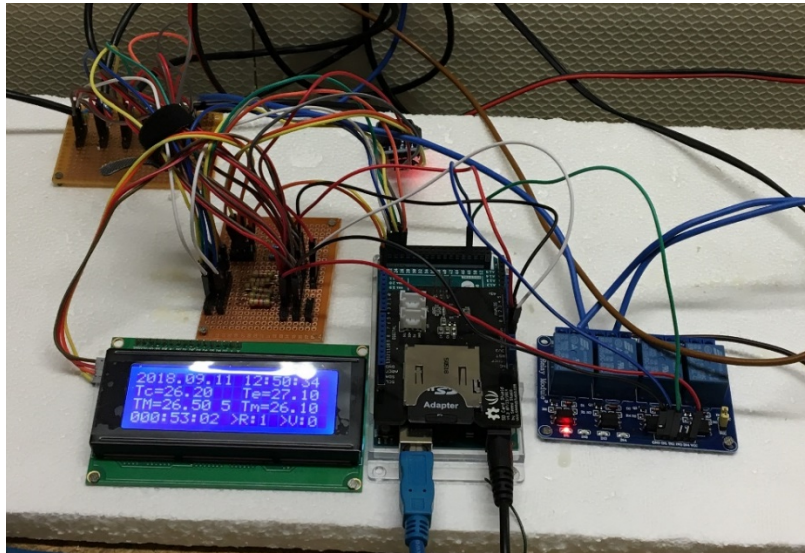
(a)
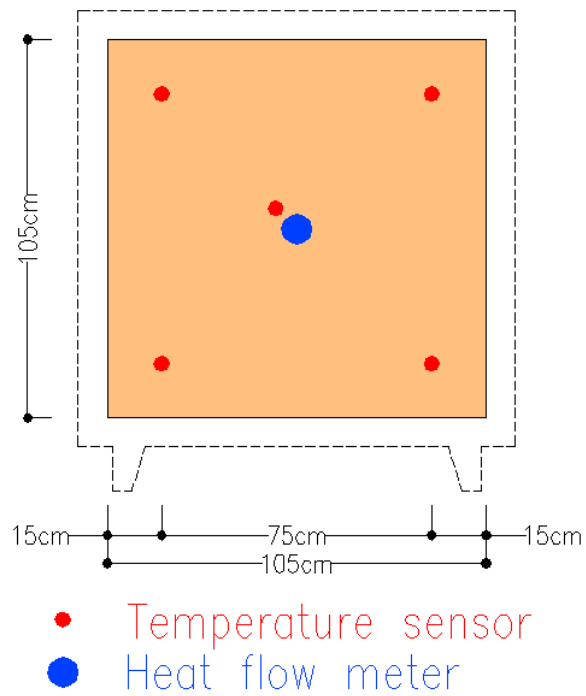
(b)

Figure 5. Details of the hardware. (a) Control unit. (b) Position of indoor sensors.

2.5 *Program developed for the acquisition*

A simple scheme of the program charged on Arduino is graphically represented in the flowchart in Figure 6. The parameters (constant during the acquisition) set for the control of the system and the variables (changing during the acquisition) used in the flowchart are explained in Table 1. It reports the initial settings for the parameters as adopted from the authors.
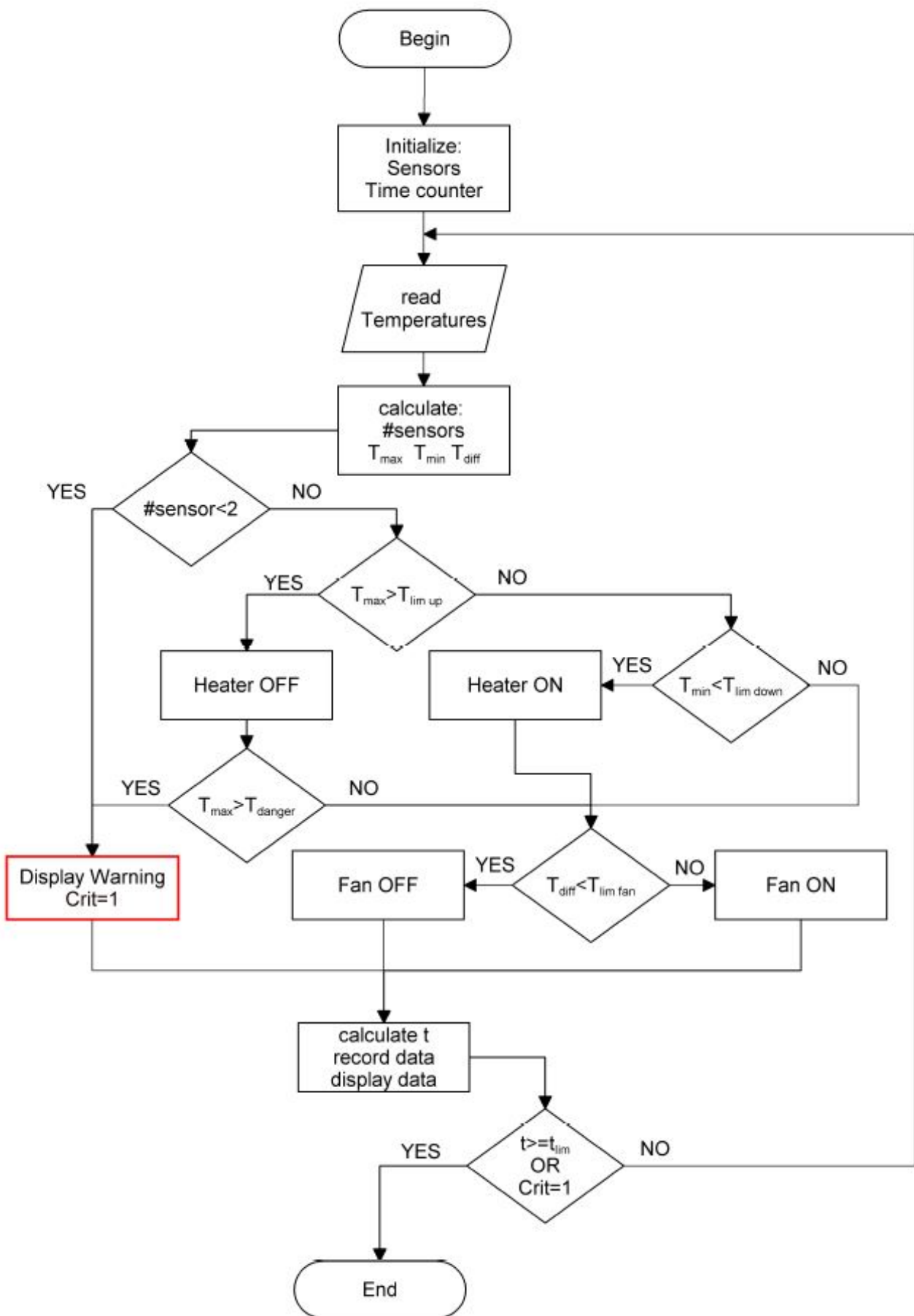
Figure 6. Flowchart showing the main blocks of the software developed for the acquisition.

Symbol	Parameter	Value
$T_{lim\ down}$	Minimum temperature	40°C
$T_{lim\ up}$	Maximum temperature	45°C
T_{danger}	Critical (potentially dangerous) temperature	55°
$T_{lim\ fan}$	Maximum temperature range between sensors	5°C
t_{lim}	Maximum test duration	72h (3days)
Symbol	**Variable**	
Crit	Emergency flag. If equal to 1, the program stops	0 or 1
T_{max}	Maximum temperature recorded by the internal sensors	-
T_{min}	Minimum temperature recorded by the internal sensors	-
T_{diff}	Difference between T_{max} and T_{min}	-
t	Time counted after the start	-

Table 1. Nomenclature of parameters and variables in Figure 6.

The main aims of the program are:

- Initialize the variables;

- Maintain the temperature between $T_{lim\ down}$ and $T_{lim\ up}$ (using the heater);

- Maintain the temperature gap lower than $T_{lim\ fan}$;

- Record all the detected data;

- Display in real-time selected data;

- Stop the system if at least one potentially dangerous criticality occurs.

Specifically, the criticalities introduced in the program are:

1. Less than two working temperature internal sensors;

2. T_{max} equal or higher than T_{danger}

In these two cases, the variable Crit is modified from 0 to 1 and then the program stops. An additional emergency system (temperature sensor with a breaker) is installed externally to Arduino. If the external system detects a temperature 2°C higher than T_{danger}, it automatically interrupts the power supply to the box. After initialization and preliminary tests, each loop was set to take 10 seconds, during the loop each variable is read or calculated and recorded on the SD card.

2.6 Data acquisition and post-processing of the acquired data

The data acquired during the test are then elaborated in order to evaluate an assessment of the conductance by using Eq. (1) according to the average method. As reported in the ISO 9869-1:2014, this method assumes that the conductance Λ can be obtained by dividing the mean density of heat flow rate (q) by the mean temperature difference (T_{si}-T_{se}), the average being taken over a long enough period of time. An estimate of the conductance Λ is then obtained by expression:

$$\Lambda = \frac{\sum_{j=1}^{n} q_j}{\sum_{j=1}^{n}(T_{si,j} - T_{se,j})} \tag{2}$$

where: j are the individual measurements and the other quantities are already defined after Eq. (1). It is worth to note that for in-situ measurement based on the average method, the ISO 9869-1:2014 the analysis shall be carried out over a period which is an integer multiple of 24 h since the method is proposed to consider the daily temperature cycle (by assuming for one cycle a duration of 24h). In our case, as reported and better explained in the following Section, the cycle considered for the evaluation of the conductance, is established as the time interval between two consecutive peaks in the temperature trend recorded in correspondence of the heat flow meter; according to this definition we will be able to considerably reduce the test duration performed with the MHB.

As far as the data acquisition is concerned, the selection of a proper time step – to be adopted for the individual measurements collecting the data to use in Eq. (2) – is a fundamental aspect. In fact, as showed in the following Section, due to cyclic turn on-turn off of the heater, the heat flow rate (Φ) and internal temperature (T_{si}) change rather rapidly in the time. To properly assess Λ, a few-minute time step should be considered even for materials with poor insulation performances. In the present work, preliminary tests for both the tested materials have been carried out to identify a proper time step. Specifically, one-tenth of heating cycle (time between two consecutive heater starting) was considered a proper time step. To uniform the tests, the

lowest obtained value (60s) has been chosen for both the material tests. For peculiar materials and different temperature ranges, similar preliminary tests should be performed.

Further aspects to take into consideration in problems facing with property assessment of hydrophilic materials, are the sample preparation operations and the preconditioning protocol. To this regard, water content and preconditioning phase could influence in an important way the final results and in order to avoid or limits these effects the current international standards, if any for the specific material to test, should be considered. Further details on the matter, are out of the scope of this paper.

3. RESULTS AND DISCUSSION

In order to validate the MHB prototype, preliminary experimental validation tests were carried out on two commercial materials. The first is a high conductance material constituting an OSB panel whereas the second is a low conductance material realizing an EPS layer. This Section summarizes the main results obtained with the MHB on two different panels, realized respectively in OSB and EPS, in terms of conductance. The identified values have been compared with those of a calibrated lab test machine. Moreover, the experimental tests have been reproduced also with a computational fluid dynamics simulation in order to further confirm the outcomes reliability.

The first experimental test reported here, has the aim to estimate the conductance of an OSB panel, commonly used, for example, in the envelope of timber rural buildings. The material was selected since it has a very low thermal resistance, or equivalently, high conductance. The outcomes from this test were used to proof the reliability of the system for study material/panel with poor insulation properties. On the other hand, the second experimental test described in a following subsection was an EPS panel, commonly used, for example, as insulation in walls and roofs of buildings. The material was selected since it has a high thermal resistance, or equivalently, low conductance. The outcomes from this test were used to proof the reliability of the system for study material/panel with good insulation properties. The two materials have been selected since they could represent a sort of inferior and superior boundaries to the expected conductance values for materials used for insulation applications. Figure 7 shows the details of the MHB set-up for both the two experimental tests.

<div align="center">(a)   (b)</div>

Figure 7. Validation tests of MHB. (a) High conductance sample. (b) Low conductance sample.

3.1 Experimental validation test on a high conductance sample

The first experimental test reported here, has the aim to estimate the conductance Λ of an OSB panel with thickness t=18mm. The outcomes from this test were used to proof the reliability of the system for study material/panel with poor insulation properties. Figure 7a shows the details of the MHB set-up.

The experimental test was performed, for 72 hours (starting around 12:00 of May 23, 2019), by considering the control parameters reported in Table 1. Figure 8 depicts the temperature behaviour for the first day of test. The reported air temperature trends are: T_{out}, outdoor temperature that is the laboratory air temperature; then T_{center}, T_{high} and T_{low} are respectively the air temperatures, inside the box, measured by the sensor at the center, high and low level of the panel. Figure 8b shows in detail, the trends of the temperatures, for 3 hours, with the addition of the measured heat flow. It is worth to notice that outdoor temperature is almost constant (around 21°C) with low variations. On the opposite, the indoor temperature ranges

between 40°C and 47°C, as expected from the setting of the internal temperature sensors. The oscillating trend on the temperatures is to attribute to the cyclic turning on-off of the thermal resistance. For the present tests the temperature difference T_{si}-T_{se} has been always abundantly higher than 10°C, suggested by the ISO 9869-1:2014. The heat flow and the air temperature trends are fundamentally in phase and the heat flow peaks occur some instant after the turning off of the heater. The conductance trend, evaluated by means of the Eq. (2), is reported for the first 24 hours of test in Figure 8c. It is worth to note that, as expected following ISO 9869-1:2014, the conductance trend converges to an asymptotical value, and the conductance value is practically stable after few hours of test. Moreover, the outcomes of this first test respect the prescriptions reported in Chapter 7 of the ISO 9869-1:2014 assuring the convergence to a proper value and close to the real. The values of the conductance after 6h, 12h, 24h and 72h (end of the test) are reported to be thorough in Table 2. For the first sample considered here, the final value after 72 hours of test is $\Lambda_{72h} = 8.51$ W/(m^2 K) and is from a practical point of view, very similar to the conductance value after 6 hours, i.e. 8.55 W/(m^2 K). If we assume as reference the conductance value after 72h of test, we can calculate the relative error E_Λ on the conductance, for a general time instant i in the following way:

$$E_{\Lambda,i} \, [\%] = (\Lambda_{72h} - \Lambda_i) / \Lambda_{72h} \times 100 \tag{3}$$

In Table 2 are reported the values of the E_Λ for the different time interval considered before. The value of the relative error is smaller than 1% already after 6 hours of testing.

For the sample investigated sample, the MHB provided a stable estimate of the conductance value after few hours from the beginning of the tests, and then, as already discussed in the introduction section, in order to obtain a preliminary value of the conductance of a material or panel, 72 hours of test duration are maybe not necessary since a sufficient level of convergence was reached even also few hours [50]. As far as the test time duration is concerned, we introduce here a convergence parameter ε useful to define, when the thermal test could be

stopped since, it reached a prescribed convergence value. For each time step of the test ε was defined in the following way:

$$\varepsilon \ [-] = (\Lambda_i - \Lambda_{i-1}) \ / \ \Lambda_i \tag{4}$$

where Λ_i is the current (i.e. relative to the actual step) value of the conductance evaluated by Eq. (2) and Λ_{i-1} is the conductance value calculated for the previous step again with Eq. (2). This parameter can be adopted to check the current convergence of the system and to stop the test is the desired threshold is reached. For the high conductance sample described here, the values of ε varying the test duration are reported in Table 2. If, for example, the convergence parameter threshold is fixed at a value of 10^{-3}, it is clear from Table 2 that just over 12 hours would have been enough to complete the thermal test with a time saving of about 60 hours.
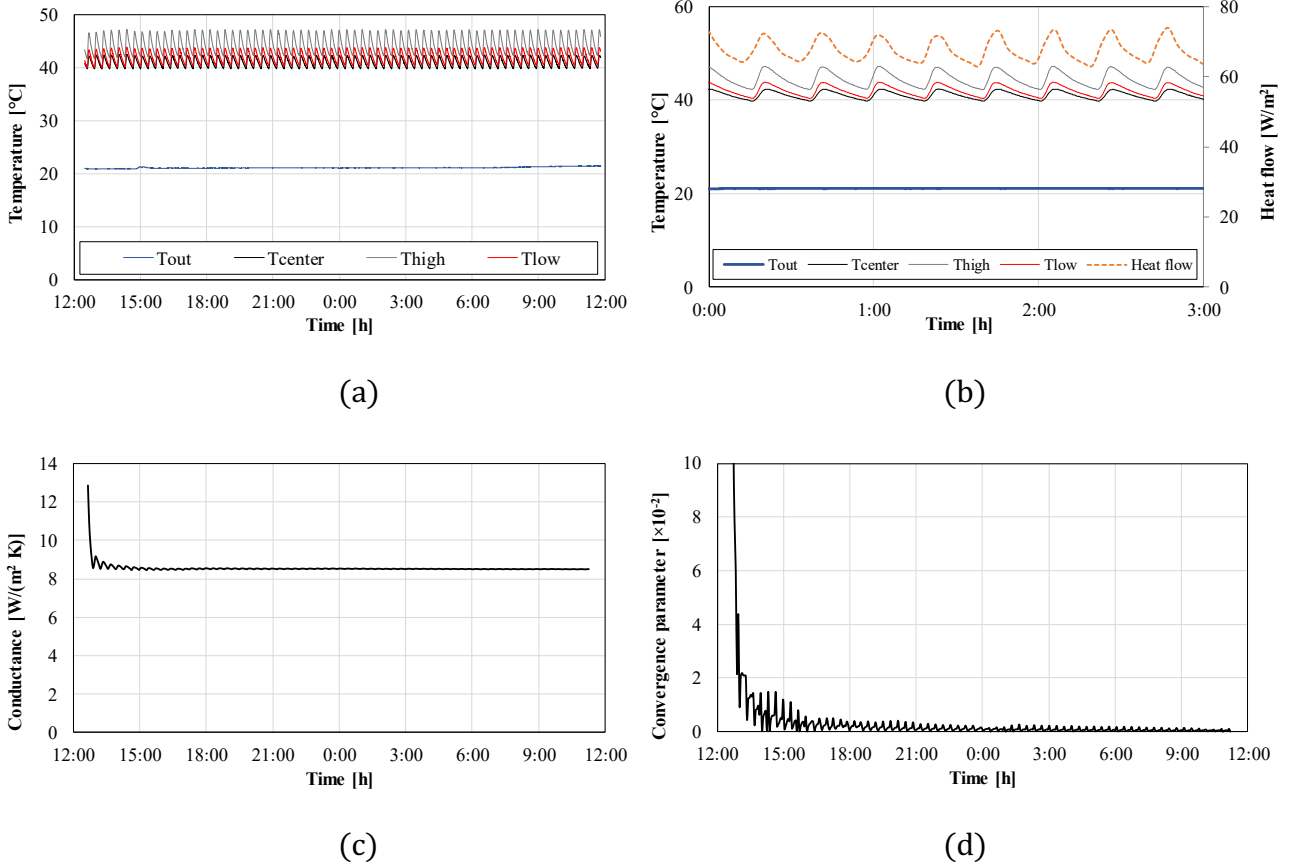
Figure 8. Trend of the main parameters obtained from the experimental test on high conductance sample. (a) Temperatures trend for the first 24 hours from the beginning (where: T_{out} is the outdoor temperature; T_{center}, T_{high} and T_{low} are respectively the indoor temperatures measured by the sensor at the center, high and low level of the panel. (b) Detail of the typical trends of temperatures and heat flow recorded during three hours of test (from 0:00 to 3:00 a.m. of the first day of the test). (c) Conductance trend for the first 24 hours from the beginning of the test. (d) Convergence parameter trend for the first 24 hours from the beginning of the test.

Parameter	after 6h	after 12h	after 24h	after 72h
High conductance sample (OSB)				
Λ [W/(m² K)]	8.55	8.53	8.52	8.51
E_Λ [%]	+0.47	+0.24	+0.12	0.00
ε [-]	0.0013	0.0011	0.0003	0.0001

Table 2. Experimental values of conductance Λ, relative error E_Λ and convergence parameter ε after 6h, 12h, 24h and 72h of test duration.

Moreover, after the thermal test with the MHB was completed, and in order to have a confirmation of the conductance value, a OSB panel sample with dimension 50cm×50cm has

been extracted from the original panel and it was tested in the guarded hot plate (GHP) apparatus of the Department of Industrial Engineering of the University of Bologna [51]. The value of the thermal conductivity provided from the GHP test, under steady state unidirectional heat flow condition, was assessed as $\lambda = 0.15$ W/(m K) equivalent to a $\Lambda = \lambda / t = 0.15/0.0185 = 8.11$W/(m^2 K). Assuming this value as the "exact" theoretical value of the material investigated, we can observe as this results is very close to the value obtained by the MHB test and provides a relative error (with respect to the theoretical value) of -4.9%, abundantly lower than the total uncertainty expected by adopting the actual procedures for material characterization estimated around 20% of the theoretical value (see Subsection 2.1).

Finally, in order to test and verify the realization and installation quality of the prototype of MHB, a thermal imaging campaign for the monitoring of external temperatures was conducted. This allowed to evaluate the distribution and homogeneity of temperatures and also the presence of thermal bridges or discontinuity due to an imperfect construction. Figure 9 shows as example an image of the the exterior surface temperature of the first sample tested.


Figure 9. Thermal image of the contour of the exterior surface temperature T$_{se}$, obtained with a thermal camera, in a generic instant of the test on the high conductance sample.

As the image highlights the temperature contour appears rather regular and without apparent discontinuities. Obviously, the image shows the thermal bridges at the specimen-MHB contact and, as expected after the CFD simulations, the effects of the discontinuity result limited to a strip of about 6-8 cm long around the perimeter of the panel sample. This is a further confirmation of the substantial limited boundary effects and of the homogeneous temperature distribution expected in the portion of sample monitored by the sensors (i.e. temperature sensors and heat flow meter). To confirm this, Figure 10a shows the assessment of the interior surface temperature distribution, provided by the CFD simulation reproducing the experimental conditions. The temperature trend resulting from the CFD simulation have been compared with the experimental results by considering the temperature recorded by the internal temperature sensors (see Figure 10b). The good agreement between the numerical results (i.e. grey dots in Figure 10b) and the experimental outcomes (i.e. orange dots in Figure 10b) confirms the reliability of the model and its ability to interpret the experimental tests. Then, in this case, the interior surface temperature contour in Figure 10a confirms the limited boundary effects and the substantial homogeneous temperature distribution expected in the central portion of the investigated specimen, where is installed the heat flow meter.
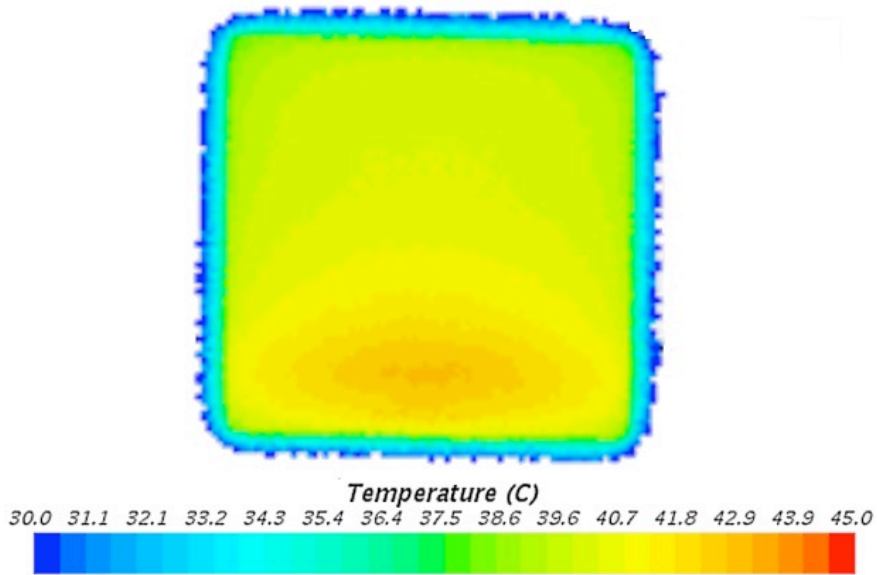
(a)
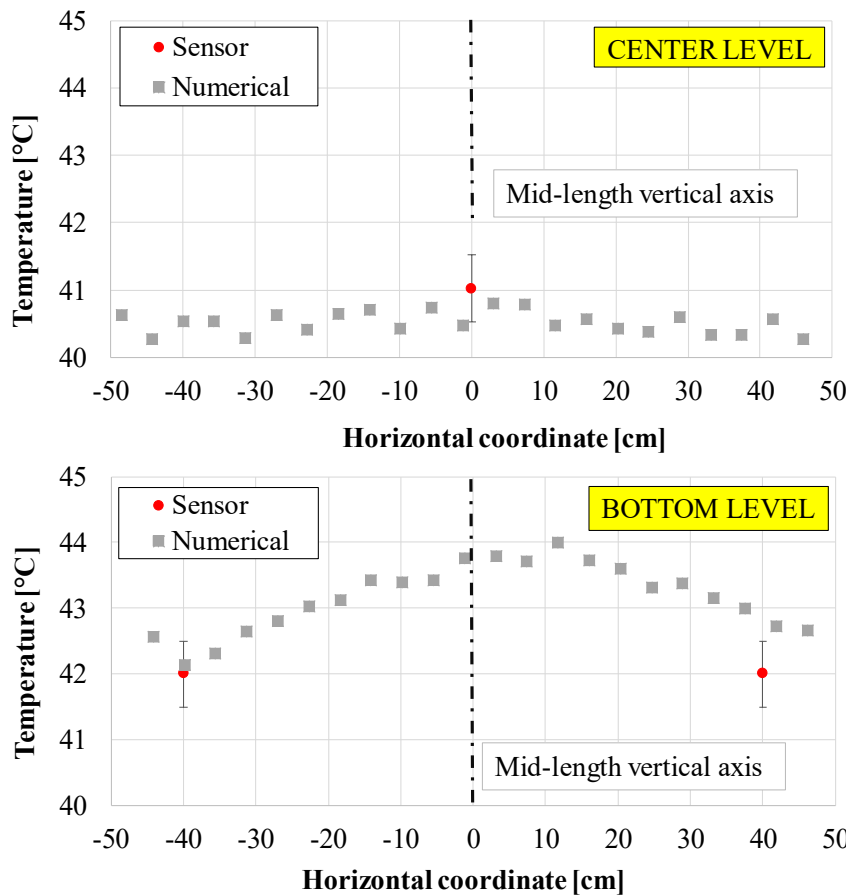
(b)

Figure 10. Outcomes of the CFD simulations of the high conductance sample. (a) Contour of the interior surface temperature T_{si}, obtained, in a generic instant of the test. (b) Comparison between numerical and experimental interior surface temperatures.

3.2 Experimental validation test on a low conductance sample

The second material experimentally tested and reported here, was an EPS panel with commercial thickness t=80mm. The outcomes from this test were used to proof the reliability of the system for study material/panel with good insulation properties. Figure 7b shows the details of the MHB set-up.

Also this second experimental testing was performed for 72 hours (starting around 16:00 of February 11, 2019). Figure 11a depicts the temperature behaviour for the first day of test (T_{out}, outdoor temperature that is the laboratory air temperature; T_{center}, T_{high} and T_{low} are respectively the air temperatures, inside the box, measured by the sensor at the center, high and low level of the panel). Figure 11b shows in detail, the trends of the temperatures, for 3 hours, with the addition of the measured heat flow. It is worth to notice that outdoor temperature is almost constant (around 13°C) variating with low rates. On the opposite, the indoor temperature ranges between 34°C and 44°C, as expected from the setting of the internal temperature sensors. The oscillating trend on the temperatures is to attribute to the cyclic turning on-off of the thermal resistance. The cycles of heat flow and air temperature have analogous period, about 45-50 minutes, and the cycles duration, as expected, is higher than the cycles duration relative to the high conductance sample, reported in Figure 8b, and long about 20 minutes. The heat flow reached peaks around 28 W/m² lower than the 55 W/m² recorded during the test on high conductance specimen. For this second sample as well, the converging conductance trend of the first 24 hours is reported in Figure 11c. Also in this case, it is worth to note that, the conductance trend converges to an asymptotical value, and the conductance value is practically stable after few hours of test as expected following ISO 9869-1:2014. Moreover, also the outcomes of this second validation test respect the prescriptions reported in Chapter 7 of the ISO 9869-1:2014 assuring the convergence to a proper value and close to the real. The values of the conductance after 6h, 12h, 24h and 72h (end of the test) have been reported in Table 2. For this sample, the final value after 72 hours of test is $\Lambda_{72h} = 0.53$ W/(m² K) and also

in this case is very similar to the conductance value after few hours (i.e. 0.56 W/(m^2 K) after 6 hours).

Also for the case of low conductance panel, the relative error (see Table 2) is rather small and around 5% already after 6 hours of testing. As far as the convergence parameter ε is concerned (see Figure 11d), if, as above, the convergence parameter threshold is fixed equal to 10^{-3}, it emerges from Table 3 that 30 hours are sufficient to complete the thermal test allowing a time saving of about 40 hours of test.

For this second panel in OSB EPS, the value of the thermal conductivity provided from the GHP test was $\lambda = 0.038$ W/(m K) equivalent to a $\Lambda = \lambda / t = 0.038/0.0798 = 0.48$ W/(m^2 K). If we assume this value as the "exact" theoretical value of the EPS investigated, we can observe as this results quite close, for a preliminary evaluation, to the value obtained by the MHB test and this last value provides a relative error, with respect to the theoretical value, of -10.0% remarkably lower than the total uncertainty expected by adopting the actual procedures for material characterization.
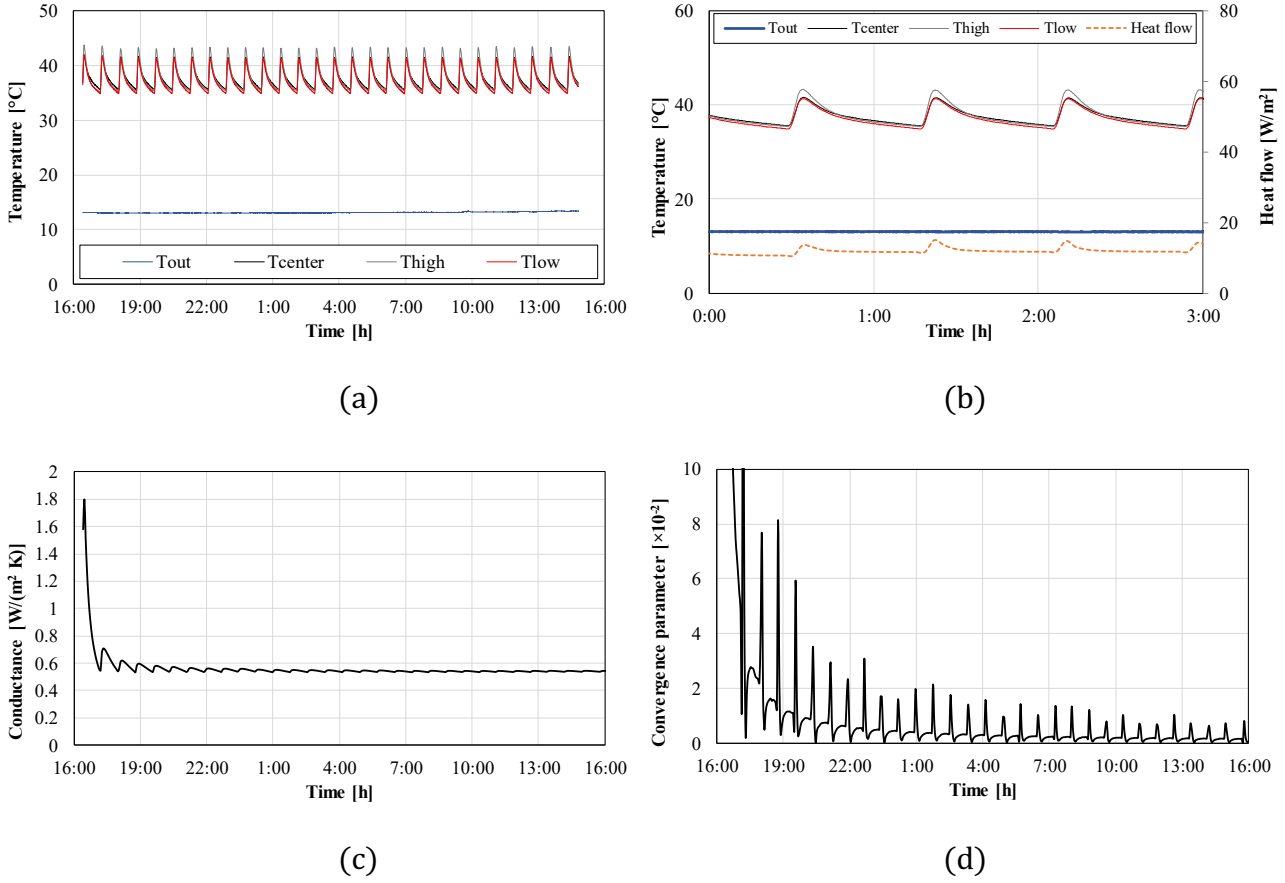
Figure 11. Trend of the main parameters obtained from the experimental test on low conductance sample. (a) Temperatures trend for the first 24 hours from the beginning (where: T_{out} is the outdoor temperature; T_{center}, T_{high} and T_{low} are respectively the indoor temperatures measured by the sensor at the center, high and low level of the panel. (b) Detail of the typical trends of temperatures and heat flow recorded during three hours of test (from 0:00 to 3:00 a.m. of the first day of the test). (c) Conductance trend for the first 24 hours from the beginning of the test. (d) Convergence parameter trend for the first 24 hours from the beginning of the test.

Parameter	after 6h	after 12h	after 24h	after 72h
Low conductance sample (EPS)				
Λ [W/(m² K)]	0.56	0.55	0.54	0.53
E_Λ [%]	+5.66	+3.77	+1.89	0.00
ε [-]	0.0052	0.0019	0.0014	0.0002

Table 3. Experimental values of conductance Λ, relative error E_Λ and convergence parameter ε after 6h, 12h, 24h and 72h of test duration.

Figure 12 shows three images of the the exterior surface temperature of the EPS sample observed during the thermal imaging campaign. The three images focus, with the spot options of the thermal camera, the local temperature around the bottom, the center and the top of the panel. As the three pictures show, the difference on the temperature are quite limited, ranging from 12.9 to 13.3 and confirming the substantial temperature homogeneity and regularity a part of the limited stripe (5-6 cm) around the perimeter were a thermal bridge surface is localized. Again, this is a further confirmation of the substantial limited boundary effects on the specimen with rather homogeneous temperature distribution expected in the area monitored by the sensors. Conversely, from the high conductance sample described in the previous subsection, in this case the external surface temperature is in general similar to the outdoor temperature in the laboratory.
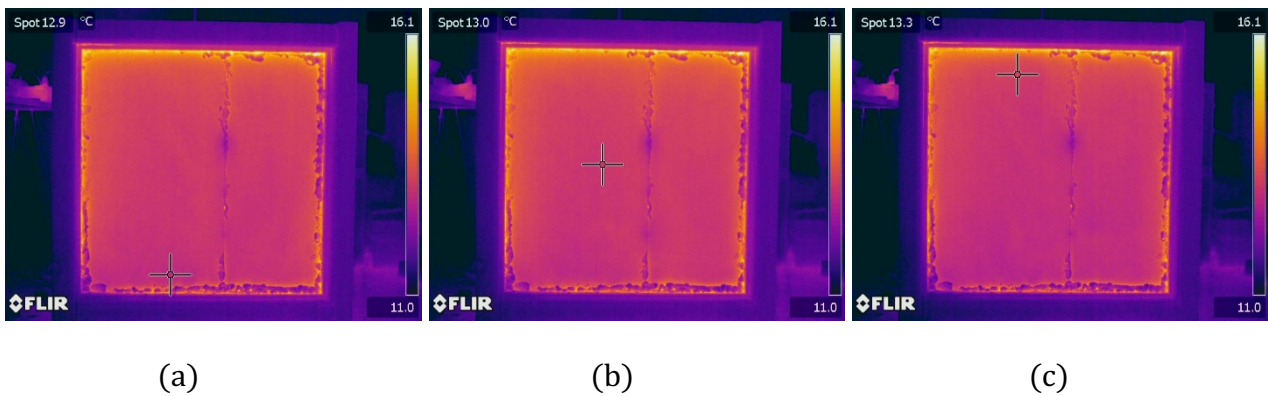

| (a) | (b) | (c) |

Figure 12. Contour of the exterior surface temperature T_{se} in a generic instant of the test on the low conductance sample with the spot options indicating the temperature around (a) the bottom, (b) the center and (c) the top of the panel.

As for the previous case, we present in Figure 13 the contour of the interior surface temperature on the low conductance sample, obtained by means of the CFD modelling.
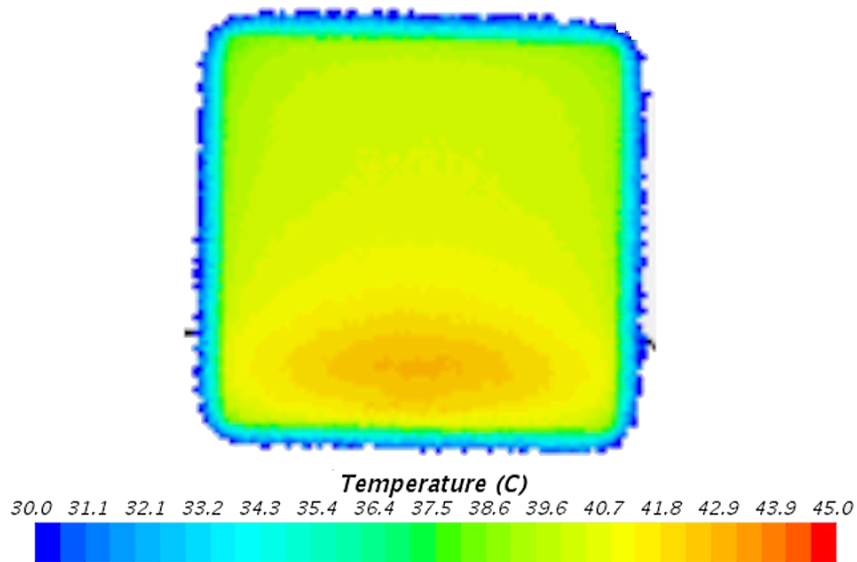
Figure 13. Contour of the interior surface temperature T_{si}, obtained from the CFD simulation, in a generic instant of the test on the low conductance sample.

The temperature trend resulting from the CFD simulation have been compared with the experimental results by considering the temperature recorded by the internal temperature sensors (see Figure 14). The good agreement between the numerical results (i.e. grey, blue and green dots respectively in Figure 14a, b and c) and the experimental outcomes (i.e. orange dots in Figure 14) confirms the reliability of the model and its ability to interpret the experimental test also for this second sample. Also for this second sample panel in EPS, the simulation confirms the limited boundary effects and the substantial homogeneous temperature distribution expected in the central portion of the investigated specimen. In this case, the low conductance of the material significantly improves the internal temperature distribution, by decreasing also the temperature picks close to the walls.
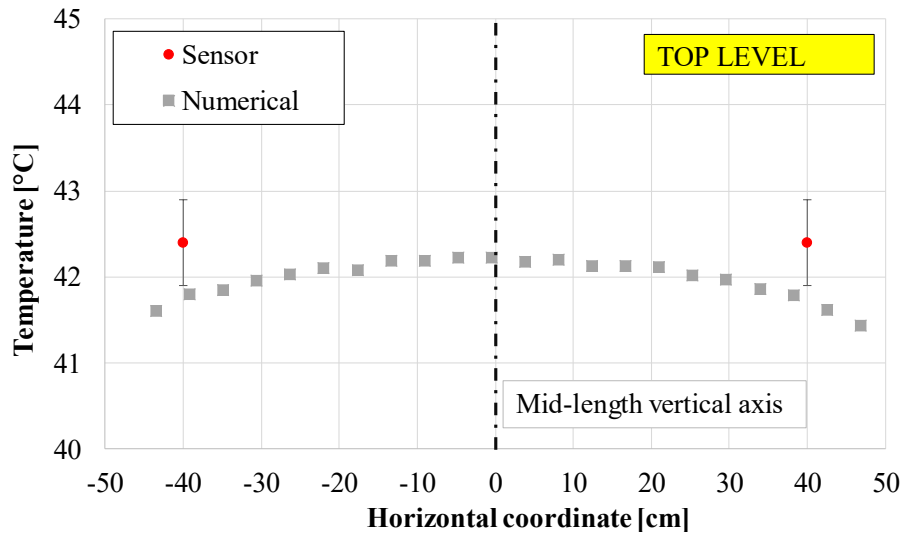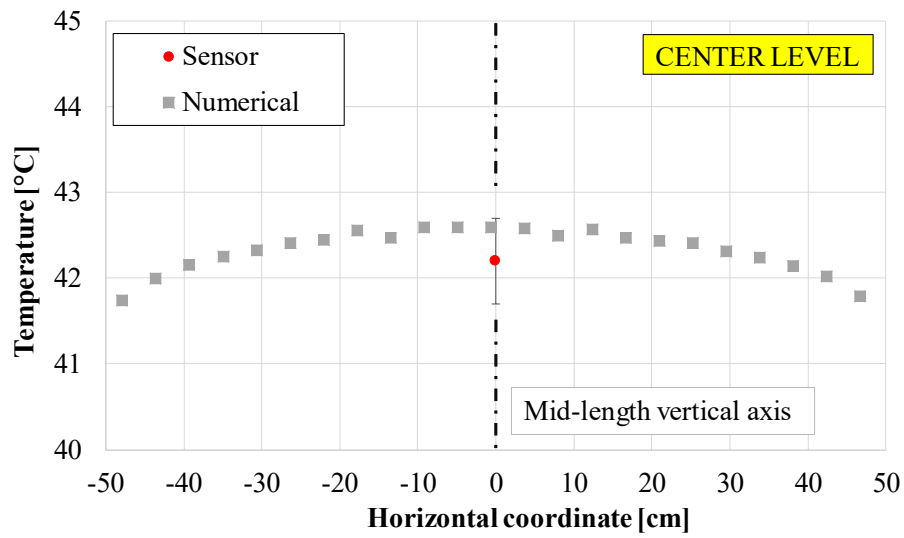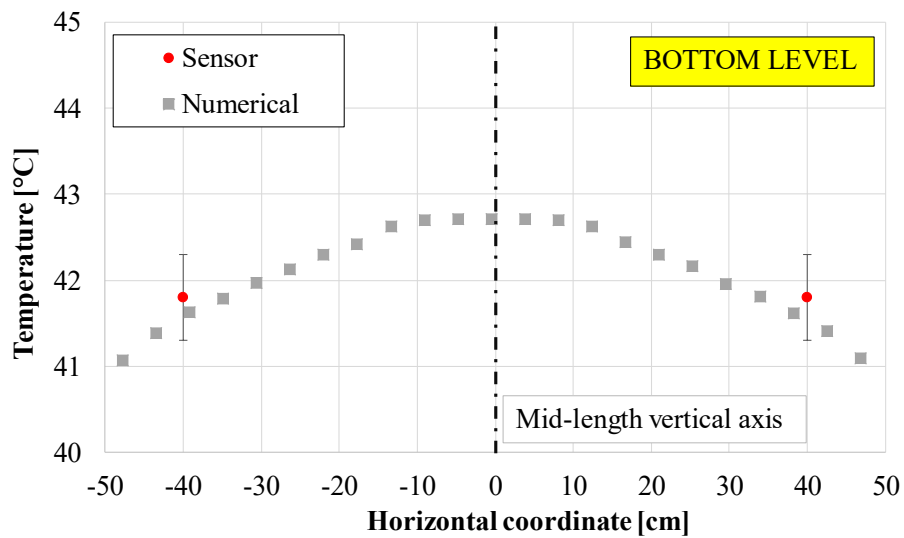
Figure 14. Comparison between the temperature profiles obtained from the CFD simulation and experimental data. Horizontal section at the level of the temperature sensors, (a) at the top (b) center and (c) bottom sensor level.

4. CONCLUSIONS

The paper shows the study, design, construction, test and validation of a prototype of a low-cost movable hot box suitable for a preliminary assessment of the thermal conductance of wall elements and insulation panels with dimensions about 1m×1m. The equipment has been thought to make preliminary test on materials – in particular agricultural and industrial waste-based materials – to consider for building thermal insulation. Since the tests suggested by regulations require voluminous and cumbersome equipment, the main idea of the project was to create a smaller-scale system.

The proposed hot box was sized mainly on the outputs of preliminary CFD simulations, then installed and finally validated using two commercial materials: a high conductance material (OSB panel) and a low conductance material (EPS). The main results in terms of conductance of the two materials have been compared with those of a calibrated lab test machine. The CFD simulation allowed to create a hot box with limited dimensions. The reduced dimensions represent an economical advantage since just one man is needed for the operability, the samples are four/five times smaller than those for the current apparatus and finally the machine is transportable and movable. The comparison of the results obtained from the proposed movable hot box and the lab-test one, shows the proposed apparatus provides results very similar to the lab test machine and with relative error remarkably lower than the uncertainty suggested by international standards and regulations. Moreover, the elevate temperature difference between surfaces (abundantly higher than 10°C suggested by the Standard ISO 9869-1:2014) and the short-period temperature cycles, allow the system to reduce the test duration for the conductance evaluation.

On the other side, the hot box cannot be used for certifications, since the regulations do not allow it and can hardly host samples and panels made with high density material (such as concrete, masonry, etc.).

Under this light, the hot box can be ideal for preliminary tests since it proves to be high cost effective, in particular if several configurations of the same material should be tested (example different orientations of the sample), or the material supply is limited or particularly expensive. Finally, even though it cannot be used for certification, the hot box provides reliable results, in short time with limited use of test materials involving one operator only.

The future developments of the research will involve the fine-tuning of the software (in particular temperature cycles settings) to reduce the test duration and the reinforcement of the structure to test heavy materials as well. In the next months the machine will be used to test several agricultural waste in different forms and configurations.

REFERENCES

[1]   United   Nations.   United   Nation   Environment   Program   2020. https://www.unenvironment.org.

[2]   European Commission. European Commission - buildings section. [Online]. 2018 n.d. https://ec.europa.eu/easme/en/section/horizon-2020-energy-efficiency/buildings.

[3]   Pérez-Lombard L, Ortiz J, Pout C. A review on buildings energy consumption information. Energy Build 2008;40:394–8. https://doi.org/10.1016/j.enbuild.2007.03.007.

[4]   Lechtenböhmer S, Schüring A. The potential for large-scale savings from insulating residential   buildings   in   the   EU.   Energy   Effic   2011;4:257–70. https://doi.org/10.1007/s12053-010-9090-6.

[5]   Cho YS, Kim JH, Hong SU, Kim Y. LCA application in the optimum design of high rise steel structures.   Renew   Sustain   Energy   Rev   2012;16:3146–53. https://doi.org/10.1016/j.rser.2012.01.076.

[6]   Cascone SM, Cascone S, Vitale M. Building insulating materials from agricultural by-products: A review. Smart Innov. Syst. Technol., vol. 163, Cascone2020: Springer; 2020, p. 309–18. https://doi.org/10.1007/978-981-32-9868-2_26.

[7]   Ardente F, Beccali M, Cellura M, Mistretta M. Building energy performance: A LCA case study   of   kenaf-fibres   insulation   board.   Energy   Build   2008;40:1–10. https://doi.org/10.1016/j.enbuild.2006.12.009.

[8]   Buratti C, Belloni E, Lascaro E, Merli F, Ricciardi P. Rice husk panels for building applications: Thermal, acoustic and environmental characterization and comparison with other innovative recycled waste materials. Constr Build Mater 2018;171:338–49. https://doi.org/10.1016/j.conbuildmat.2018.03.089.

[9]   Barreca F, Martinez Gabarron A, Flores Yepes JA, Pastor Pérez JJ. Innovative use of giant reed and cork residues for panels of buildings in Mediterranean area. Resour Conserv Recycl 2019;140:259–66. https://doi.org/10.1016/j.resconrec.2018.10.005.

[10] Binici H, Aksogan O. Insulation material production from onion skin and peanut shell fibres, fly ash, pumice, perlite, barite, cement and gypsum. Mater Today Commun 2017;10:14–24. https://doi.org/10.1016/j.mtcomm.2016.09.004.

[11] Alyousef R, Benjeddou O, Soussi C, Khadimallah MA, Jedidi M. Experimental Study of New Insulation Lightweight Concrete Block Floor Based on Perlite Aggregate, Natural Sand, and Sand Obtained from Marble Waste. Adv Mater Sci Eng 2019;2019. https://doi.org/10.1155/2019/8160461.

[12] Asdrubali F, D'Alessandro F, Schiavoni S. A review of unconventional sustainable building insulation materials. Sustain Mater Technol 2015;4:1–17. https://doi.org/10.1016/j.susmat.2015.05.002.

[13] Heidari MD, Mathis D, Blanchet P, Amor B. Streamlined life cycle assessment of an innovative bio-based material in construction: A case study of a phase change material panel. Forests 2019;10. https://doi.org/10.3390/f10020160.

[14] Fabiani C, Pisello AL, Barbanera M, Cabeza LF. Palm oil-based bio-PCM for energy efficient building applications: Multipurpose thermal investigation and life cycle assessment. J Energy Storage 2020;28. https://doi.org/10.1016/j.est.2019.101129.

[15] International Standard Organization. ISO 9869-1:2014 Thermal insulation — Building elements — In-situ measurement of thermal resistance and thermal transmittance — Part 1: Heat flow meter method 2014:36.

[16] International Standard Organization. ISO 6946:2017 Building components and building elements — Thermal resistance and thermal transmittance — Calculation methods 2017:40.

[17] Barbaresi A, Bovo M, Torreggiani D. The dual influence of the envelope on the thermal performance of conditioned and unconditioned buildings. Under Rev 2020.

[18] Barbaresi A, Dallacasa F, Torreggiani D, Tassinari P. Retrofit interventions in non-conditioned rooms: calibration of an assessment method on a farm winery. J Build

Perform Simul 2017;10:91–104. https://doi.org/10.1080/19401493.2016.1141994.

[19]   Torreggiani D, Barbaresi A, Dallacasa F, Tassinari P. Effects of different architectural solutions on the thermal behaviour in an unconditioned rural building. The case of an Italian winery. J Agric Eng 2018;49. https://doi.org/10.4081/jae.2018.779.

[20]   European Commitee for Standardization. CEN - EN ISO 8990 Thermal Insulation - Determination of Steady-State Thermal Transmission Properties - Calibrated and Guarded Hot Box 1996.

[21]   ASTM International. ASTM C518 - 17 Standard Test Method for Steady-State Thermal Transmission Properties by Means of the Heat Flow Meter Apparatus 2017.

[22]   Gounni A, Mabrouk MT, El Wazna M, Kheiri A, El Alami M, El Bouari A, et al. Thermal and economic evaluation of new insulation materials for building envelope based on textile waste.   Appl   Therm   Eng   2019;149:475–83. https://doi.org/10.1016/j.applthermaleng.2018.12.057.

[23]   Ricciu R, Galatioto A, Besalduch LA, Desogus G, Pilla L Di. Building wall heat capacity measurement through flux sensors. J Sustain Dev Energy, Water Environ Syst 2019;7:44–56. https://doi.org/10.13044/j.sdewes.d6.0234.

[24]   Meng X, Gao Y, Wang Y, Yan B, Zhang W, Long E. Feasibility experiment on the simple hot box-heat flow meter method and the optimization based on simulation reproduction. Appl   Therm   Eng   2015;83:48–56. https://doi.org/10.1016/j.applthermaleng.2015.03.010.

[25]   Meng X, Luo T, Gao Y, Zhang L, Shen Q, Long E. A new simple method to measure wall thermal transmittance in situ and its adaptability analysis. Appl Therm Eng 2017;122:747–57. https://doi.org/10.1016/j.applthermaleng.2017.05.074.

[26]   Roque E, Vicente R, Almeida RMSF, Mendes da Silva J, Vaz Ferreira A. Thermal characterisation of traditional wall solution of built heritage using the simple hot box-heat flow meter method: In situ measurements and numerical simulation. Appl Therm

Eng 2020;169:114935. https://doi.org/10.1016/j.applthermaleng.2020.114935.

[27] Zach J, Hroudová J, Brožovský J, Krejza Z, Gailius A. Development of thermal insulating materials on natural base for thermal insulation systems. Procedia Eng., vol. 57, Elsevier Ltd; 2013, p. 1288–94. https://doi.org/10.1016/j.proeng.2013.04.162.

[28] Briga-Sá A, Nascimento D, Teixeira N, Pinto J, Caldeira F, Varum H, et al. Textile waste as an alternative thermal insulation building material solution. Constr Build Mater 2013;38:155–60. https://doi.org/10.1016/j.conbuildmat.2012.08.037.

[29] Schiavoni S, D'Alessandro F, Bianchi F, Asdrubali F. Insulation materials for the building sector: A review and comparative analysis. Renew Sustain Energy Rev 2016;62:988–1011. https://doi.org/10.1016/j.rser.2016.05.045.

[30] Reif M, Zach J, Hroudová J. Studying the Properties of Particulate Insulating Materials on Natural Basis. Procedia Eng., vol. 151, Elsevier Ltd; 2016, p. 368–74. https://doi.org/10.1016/j.proeng.2016.07.390.

[31] Cetiner I, Shea AD. Wood waste as an alternative thermal insulation for buildings. Energy Build 2018;168:374–84. https://doi.org/10.1016/j.enbuild.2018.03.019.

[32] International Standard Organization. ISO 9869-2:2018 Thermal insulation — Building elements — In-situ measurement of thermal resistance and thermal transmittance — Part 2: Infrared method for frame structure dwelling 2018.

[33] Ficco G, Iannetta F, Ianniello E, D'Ambrosio Alfano FR, Dell'Isola M. U-value in situ measurement for energy diagnosis of existing buildings. Energy Build 2015;104:108–21. https://doi.org/10.1016/j.enbuild.2015.06.071.

[34] Cesaratto PG, De Carli M, Marinetti S. Effect of different parameters on the in situ thermal conductance evaluation. Energy Build 2011;43:1792–801. https://doi.org/10.1016/j.enbuild.2011.03.021.

[35] Desogus G, Mura S, Ricciu R. Comparing different approaches to in situ measurement of building components thermal resistance. Energy Build 2011;43:2613–20.

https://doi.org/10.1016/j.enbuild.2011.05.025.

[36] Asdrubali F, D'Alessandro F, Baldinelli G, Bianchi F. Evaluating in situ thermal transmittance of green buildings masonries: A case study. Case Stud Constr Mater 2014;1:53–9. https://doi.org/10.1016/j.cscm.2014.04.004.

[37] Ahmad A, Maslehuddin M, Al-Hadhrami LM. In situ measurement of thermal transmittance and thermal resistance of hollow reinforced precast concrete walls. Energy Build 2014;84:132–41. https://doi.org/10.1016/j.enbuild.2014.07.048.

[38] Evangelisti L, Guattari C, Gori P, Vollaro R. In Situ Thermal Transmittance Measurements for Investigating Differences between Wall Models and Actual Building Performance. Sustainability 2015;7:10388–98. https://doi.org/10.3390/su70810388.

[39] Cesaratto PG, De Carli M. A measuring campaign of thermal conductance in situ and possible impacts on net energy demand in buildings. Energy Build 2013;59:29–36. https://doi.org/10.1016/j.enbuild.2012.08.036.

[40] Trethowen H. Measurement errors with surface-mounted heat flux sensors. Build Environ 1986;21:41–56. https://doi.org/10.1016/0360-1323(86)90007-7.

[41] European Commission. EPBD - Recast of the Directive on the energy performance of buildings (2010/31/EU). 14 December 2010 2010.

[42] International Standard Organization. ISO 8301:1991/AMD 1:2010 Thermal insulation — Determination of steady-state thermal resistance and related properties — Heat flow meter apparatus — Amendment 1 2010.

[43] European Commitee for Standardization. EN12667:2001 Thermal performance of building materials and products - Determination of thermal resistance by means of guarded hot plate and heat flow meter methods - Products of high and medium thermal resistance 2001.

[44] European Commitee for Standardization. EN ISO 7345:2018 Thermal performance of buildings and building components - Physical quantities and definitions (ISO 7345:2018)

2018.

[45]   Autodesk. Autodesk Inventor 2018.

[46]   Siemens. Star CCM+ 2019.

[47]   Santolini E, Barbaresi A, Torreggiani D, Tassinari P. Numerical simulations for the optimisation of ventilation system designed for wine cellars. J Agric Eng 2019;50:180–90. https://doi.org/10.4081/jae.2019.952.

[48]   Di Sabatino S, Buccolieri R, Pulvirenti B, Britter R. Simulations of pollutant dispersion within idealised urban-type geometries with CFD and integral models. Atmos Environ 2007;41:8316–29. https://doi.org/10.1016/j.atmosenv.2007.06.052.

[49]   Carlesi Instruments. Thermozig BLE 2019. http://www.carlesistrumenti.eu/diagnosi-edilizia/analisi-energetica/termoflussimetri.html (accessed March 7, 2020).

[50]   Gaspar K, Casals M, Gangolells M. Review of criteria for determining HFM minimum test duration. Energy Build 2018;176:360–70. https://doi.org/10.1016/j.enbuild.2018.07.049.

[51]   Baldinelli G, Bianchi F, Gendelis S, Jakovics A, Morini GL, Falcioni S, et al. Thermal conductivity measurement of insulating innovative building materials by hot plate and heat flow meter devices: A Round Robin Test. Int J Therm Sci 2019;139:25–35. https://doi.org/10.1016/j.ijthermalsci.2019.01.037.